# A CURVILINEAR BOUSSINESQ MODEL AND ITS APPLICATION

Fengyan Shi , James T. Kirby, Robert A. Dalrymple,[1]and Qin Chen[2]

**Abstract:** In this paper, a curvilinear Boussinesq model is further improved in order to be used in more practical applications. Firstly, the energy dissipation due to wave breaking is considered by introducing an eddy viscosity term into momentum equations. Secondly, the slot technique is introduced into the curvilinear model for simulations of wave run-up/run-down in swash zones. Thirdly, Smagorinsky subgrid lateral turbulent mixing is utilized to account for the effect of the resultant eddy viscosity on the wave-generated underlying flow. In addition, a TMA spectral wave maker is implemented in the model for simulations of irregular waves. Finally, the model is used to simulate wave propagation in Ponce de Leon Inlet. Model/data comparisons show the fully nonlinear Boussinesq model give accurate results for nonlinear wave transformation over irregular bathymetry. It is also shown that the curvilinear model is an efficient model for wave computations in large computational regions with complex geometry.

## INTRODUCTION

Boussinesq models for surface gravity waves have been shown to provide an accurate tools for simulations of wave evolution in coastal regions. Recent advances both in the Boussinesq equations with improved dispersion relationships in relatively deep water (see, e.g., Madsen and Sørensen, 1992; Nwogu, 1993; Wei *et al.,* 1995 ) and in computer technology allow the use of Boussinesq models in large nearshore regions. The incorporation of wave breaking and wave runup into Boussinesq models (Karambas and Koutitas, 1992; Schäffer *et al.*,, 1993; Madsen *et al.*, 1997; and Kennedy *et al.,* 2000) also allows these models to be applied to surf zones and swash zones. In addition, Boussinesq models with either structured or unstructured computational grids were developed for computations in complex nearshore domains. Sørensen and Sørensen (2000) carried out a finite element Boussinesq model based on the equations derived by Madsen and Sørensen (1992). A finite element Boussinesq model and a finite difference curvilinear Boussinesq model based on Beji and Nadaoka's equations were developed by Li *et al.* (1999, 2001). Shi *et al.*(2001) developed a finite difference Boussinesq

[1]Center for Applied Coastal Research, Ocean Engineering Lab, University of Delaware, Newark, DE 19716, USA. fyshi@coastal.udel.edu

[2]Department of Civil Engineering, University of South Alabama, Mobile, AL 36688, USA. qchen@jaguar1.usouthal.edu

model in generalized curvilinear coordinates based on fully nonlinear Boussinesq equations (Wei *et al.,* 1995). Spatially varying and boundary-fitted grids were adopted in the case studies of the model which show that, compared to the Cartesian version of Boussinesq model, the curvilinear model has better efficiency and capability to deal with complex geometry in some complicated nearshore domains.

Many practical applications of Boussinesq models involve calculations of wave breaking, wave run-up/run-down, wave-induced currents and random wave propagations. In order to use the curvilinear Boussinesq model in more practical applications, several improvements are made in the present paper based on the existing curvilinear Boussinesq model developed by Shi *et al.* (2001). The energy dissipation due to wave breaking is considered by introducing an eddy viscosity term into momentum equations. Smagorinsky-type subgrid terms are employed to model the horizontally distributed eddy viscosity resulting from subgrid turbulent processes. To simulate swash motions, a slot technique is implemented in the model for simulations of wave run-up and run-down. A TMA shallow water wave spectrum (Bouws *et al.*, 1985) and a wrapped normal directional spreading function (Borgman, 1984) are used for directional spectral wave generations in the present model.

To demonstrate the capability and accuracy of the present model to calculate nonlinear waves in complicated domain, the model is then used in wave simulations in Ponce De Leon Inlet, Florida where a 1:100-scale physical model has been conducted at the U.S. Army Engineer Research & Development Center. The self-adaptive grid generation method (Brackbill *et al., 1982*) is adopted to generate a nonorthogonal grid which has a good resolution near the shoreline and fits well the complicated boundaries like the jetty and curved coastlines. The simulated waves include monochromatic waves, spectral waves, normally incident waves and obliquely incident waves. The calculated wave heights are compared with measured data at gauge points in two measurement arrays. For strong nonlinear wave cases, comparisons of skewness and asymmetry of waves are made between numerical results and measurement data. It is shown that the curvilinear model is efficient and accurate model for nonlinear wave simulations in large complicated coastal areas.

## CURVILINEAR BOUSSINESQ MODEL

### Governing equations in generalized curvilinear coordinates

The fully nonlinear Boussinesq equations (Wei *et al., 1995*) can be written in the tensor-invariant forms after a generalized coordinate transformation (Shi *et al.*, 2001):

$$\beta\eta_t + \frac{1}{\sqrt{g_0}}\frac{\partial}{\partial x^k}(\sqrt{g_0}M^k) = 0, \tag{1}$$

$$M^k = \Lambda\{(h+\eta)u^k + (h+\eta)[\frac{z_\alpha^2}{2} - \frac{1}{6}(h^2 - h\eta + \eta^2)][\frac{1}{\sqrt{g_0}}\frac{\partial}{\partial x^l}(\sqrt{g_0}u^l)]\}^k$$

$$+(h+\eta)[z_\alpha+\frac{1}{2}(h-\eta)][\frac{1}{\sqrt{g_0}}\frac{\partial}{\partial x^l}(\sqrt{g_0}hu^l)]!^k\}. \tag{2}$$

$$\frac{\partial u^k}{\partial t}+g\eta!^k+u^l u^k_{,l}+V_1^k+V_2^k+R_b^k+R_s^k=0, \tag{3}$$

where $k,l=1$ and 2; $(u^1,u^2)$ are the contravariant components of a reference velocity at a reference elevation $z_\alpha$; $(x^1,x^2)$ are new independent variables in the transformed image domain; $\beta$ and $\Lambda$ are two dimensionless multipliers introduced for the treatment of shoreline run-up. $\sqrt{g_0}$ is the Jacobi value; $()_k$ represents the covariant spatial derivative while $!^k$ represents the contravariant spatial derivative. $V_1^k$ and $V_2^k$ are the dispersive Boussinesq terms that can be found in Shi *et al.* (2001).

In equation (3), $R_b^k$ and $R_s^k$ represent the breaking terms and the subgrid mixing terms respectively.

**Energy dissipation due to wave breaking and subgrid mixing**

The energy dissipation due to wave breaking in shallow water is modeled by using the momentum mixing terms which can be written in a general form as

$$\frac{1}{H}\mathrm{d}iv(H\nu\mathbf{D}) \tag{4}$$

where $\nu$ is the eddy viscosity localized on the front face of the breaking wave (See Kennedy *et al.*, 1999 and Chen *et al.*, 1999); $\mathbf{D}$ is the rate-of-strain tensor defined by

$$\mathbf{D}=\frac{1}{2}[\mathrm{g}rad\mathbf{u}+(\mathrm{g}rad\mathbf{u})^T] \tag{5}$$

in which $(\mathrm{g}rad\mathbf{u})^T$ is the transpose of $\mathrm{g}rad\mathbf{u}$. The tensor-invariant forms of the diffusion terms in generalized curvilinear coordinates can be expressed as

$$R_b^k=\frac{1}{H\sqrt{g_0}}\frac{\partial\sqrt{g_0}\nu HD^{ki}}{\partial x^i}+\nu D^{ji}\Gamma^k_{ji} \tag{6}$$

where $\Gamma^k_{ji}$ represents the Christoffel symbol of the second kind and

$$D^{ij}=\frac{1}{2}(g^{kj}u^i_{,k}+g^{ki}u^j_{,k}) \tag{7}$$

The subgrid mixing terms are in the same form as shown in (4) except that $\nu$ should be replace by the eddy viscosity due to the subgrid turbulence $\nu_s$:

$$\nu_s=c\sqrt{g_0}|T|=c\sqrt{g_0}(T^{ij}T_{ij})^{1/2} \tag{8}$$

where $T$ is the rate-of-strain tensor of the velocity of the wave-generated current $\mathbf{U}$ and can be written as

$$\mathbf{T}=\frac{1}{2}[\mathrm{g}rad\mathbf{U}+(\mathrm{g}rad\mathbf{U})^T] \tag{9}$$

### Slot technique

Following the rectangular version of the fully nonlinear Boussinesq model (Chen *et al.* ,1999), a slot technique is implemented in the curvilinear model. The dimensionless multipliers $\beta$ and $\Lambda$ in equation (1) and (2) are defined exactly as in Chen *et al.* (1999). The implementation is also the same as in the rectangular version except that the slots are always along the curvilinear coordinate lines.

### Implementation of TMA spectrum wavemaker

A TMA shallow water wave spectrum (Bouws *et al.*, 1985) and a wrapped-normal directional spreading function (Borgman, 1984) are used in the present model. The combined the spectrum function can be expressed as

$$S(f,h,\theta) = E_{TMA}G(\theta) \tag{10}$$

In (10), $E_{TMA}$ is the TMA shallow water frequency distribution as follows

$$E_{TMA}(f,h) = \alpha g^2 f^{-5}(2\pi)^{-4}\Phi(2\pi f,h)e^{-5/4(f/f_p)^{-4}}\gamma^{exp[-(f/f_p-1)^2/2\sigma^2]} \tag{11}$$

in which $f_p$ is the peak frequency. $\alpha, \Phi$ and $\sigma$ are coefficients and can be found in Bouws *et al.* (1985). $\gamma$ presents frequency spreading parameter which is used in both the laboratory experiments and the present numerical simulations.

$G(\theta)$ is the wrapped normal directional spreading function written as

$$G(\theta) = \frac{1}{2\pi} + \frac{1}{\pi}\sum_{n=1}^{N} exp[-\frac{(n\sigma_\theta)^2}{2}]cosn\theta \tag{12}$$

where $\sigma_\theta$ denotes circular deviation of the wrapped normal spreading function. To avoid the underflow, $N \leq 10/\sigma_\theta$ in the present paper. The directional spectrum is divided into several components with random phases and equal energy at each frequency block. The source function technique (Wei, *et al.*, 1999) is then used for each component.

## APPLICATION

As a practical application, wave simulations in Ponce de Leon Inlet are carried out in the present paper. The bathymetry of Ponce de Leon Inlet is represented in a 1:100-scale physical model located at the U.S. Army Engineer Research & Development Center. The topography is derived from a 1994 airborne laser (lidar) survey and partial measurements in the physical model. Wave data were collected with 30 wave gauges, shown in Figure 1 (circles), at a sampling frequency of 25 Hz. Twenty-four gauges were placed in two linear arrays. One array was positioned across the outer lobe of the ebb shoal (offshore array) and another closer to shore (nearshore array). Smith and Harkins (1997) used three numerical wave models, RCPWAVE, REF/DIF, and STWAVE, in these studies and made evaluations of the three models against the measured data. It was found that model errors increase markedly with increases in wave nonlinearity because the three numerical models rely on linear wave theory.

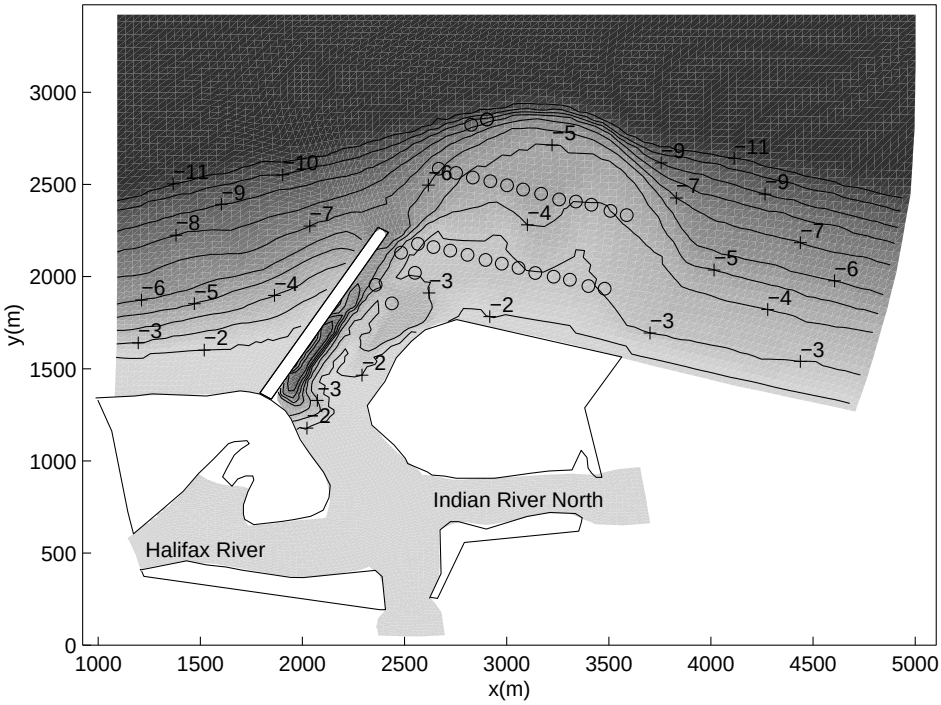


**Fig. 1. Bathymetry at Ponce de Leon Inlet (Depths in meters).**

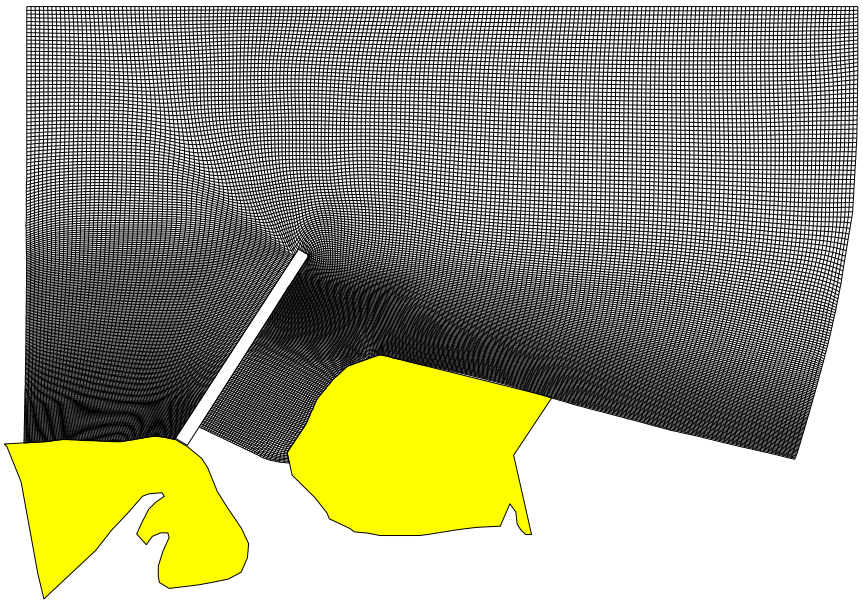

**Fig. 2. Computational grid.**

**Curvilinear grid and model setup**

A boundary-fitted grid is generated using a Matlab code for grid generation developed at the Center for Applied Coastal Research, University of Delaware and is shown in Figure 2. The grid dimension is $401 \times 781$. The finer resolution is used near the jetty, coastlines and the inlet in order to resolve structures and short waves in shallow water. The minimum grid size is $1.39m$ near the shoreline on right side of the jetty and the maximum grid size in the offshore direction is $5.4m$.

To minimize reflected waves from lateral boundaries and the artificial boundary inside the inlet, sponge layers are put at the boundaries as in the laboratory experiments. Relatively thin (five points) and weak sponge layers are also used around the jetty to partially absorb waves. It is found that the thin sponge layers do not affect significantly the results at the measurement gauges.

Totally 18 cases either with monochromatic input waves or with TMA spectral waves are carried out in this study. Table 1 presents a list of incident wave conditions generated in the numerical model. There are totally 26 cases done in the physical model. We generally choose a typical case from the cases with the similar incident wave conditions. We also skip the cases with very large wave height in which we find some difficulties to generate ideal incident waves by using the wave maker.

The model is firstly calibrated using the measurement data at the two gauges in front of the wave-maker. Each case is run for about 150 — 200 wave periods.

**Table 1.Cases with different incident wave conditions**

| Case | H(m) | T(sec) | $\theta$(deg) | $\gamma$ | $\sigma_m(deg)$ |
|---|---|---|---|---|---|
| 01 | 0.95 | 8 | 0 | Mono | |
| 02 | 1.01 | 8 | 0 | 3.3 | 30 |
| 03 | 1.15 | 8 | -30 | Mono | |
| 04 | 1.05 | 8 | -30 | 3.3 | 30 |
| 05 | 1.05 | 8 | 30 | 3.3 | 30 |
| 06 | 1.32 | 8 | 30 | Mono | |
| 07 | 0.93 | 10 | 0 | Mono | |
| 08 | 0.95 | 10 | 0 | 5.0 | 20 |
| 09 | 0.87 | 10 | -30 | Mono | |
| 10 | 0.93 | 10 | -30 | 5.0 | 20 |
| 11 | 0.74 | 10 | 30 | Mono | |
| 12 | 0.84 | 10 | 30 | 5.0 | 20 |
| 13 | 0.78 | 15 | 0 | Mono | |
| 14 | 0.98 | 15 | 0 | 7.0 | 10 |
| 15 | 0.90 | 15 | -30 | Mono | |
| 16 | 0.73 | 15 | -30 | 7.0 | 10 |
| 17 | 0.77 | 15 | 30 | Mono | |
| 18 | 0.76 | 15 | 30 | 7.0 | 10 |

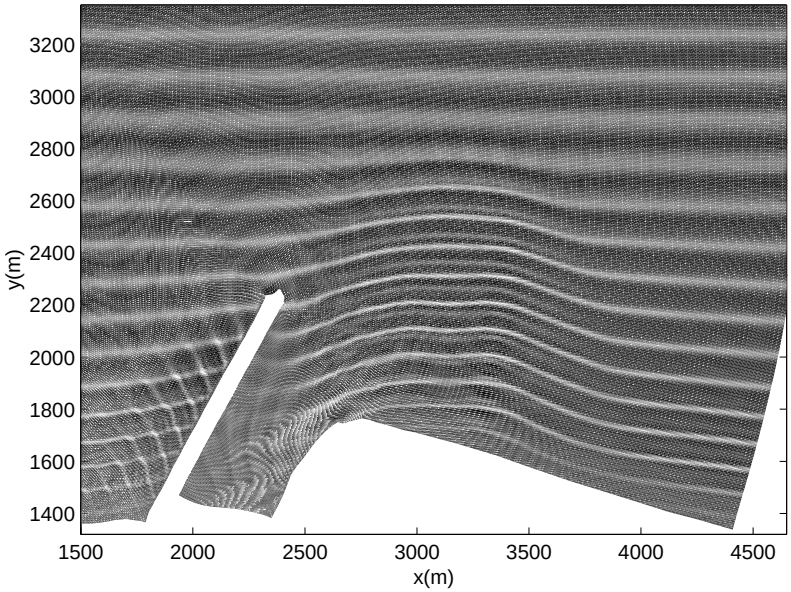


**Fig. 3. Snapshot of wave surface elevation (Case 13)**

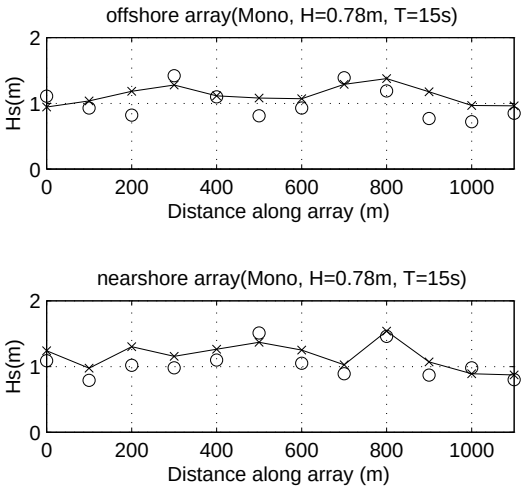


**Fig. 4. Wave height comparisons (Case 13. Circle: data, solid line: model).**

### Model results and model/data comparisons

The cases listed on Table 1 include monochromatic waves and random waves with normal incidence or oblique incidence. Here we only show some typical cases that demonstrate capabilities of the present model to calculate nonlinear waves and to deal with the complex geometry.

Figure 3 shows a snapshot of surface elevations of normally incident monochromatic waves with a period of 15 second (Case 13). This long period wave case shows a strong nonlinear wave property which is represented by the obvious second harmonic waves in the nearshore region. Figure 3 also shows clearly the wave reflection on the upward side of the jetty, wave diffraction on the leeward side, wave scattering from the tip of the jetty and refractive wave focusing in the area to the right of the inlet mouth. Figure 4 shows the comparisons of wave heights

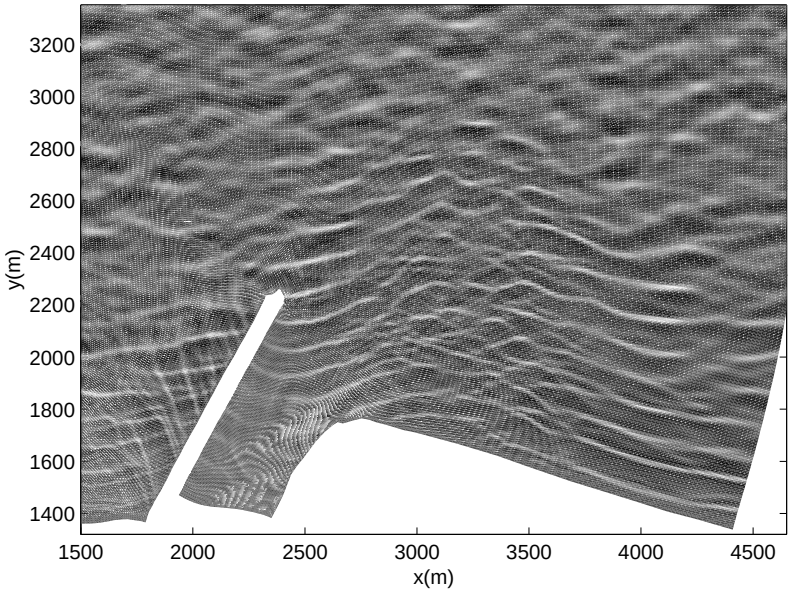


**Fig. 5. Snapshot of wave surface elevation (Case 14)**

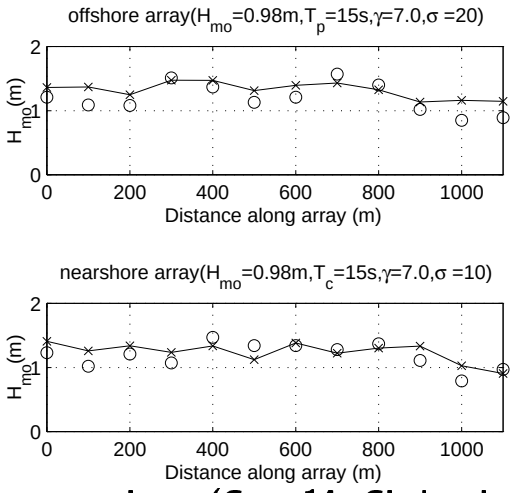


**Fig. 6. Wave height comparisons (Case 14. Circle: data, solid line:model).**

between model results and measurement data. It is shown that the Boussinesq model predicts well the bathymetric influences on wave transformation and wave focusing feature.

A spectral wave case with the peak period of 15 seconds (Case 14) is shown in figure 5. The figure presents some typical phenomena of directional spectral waves, like that the short crest waves offshore become long crest waves as they are propagating to the shoreline, wave refraction and focusing are less obvious than those in the monochromatic wave cases. The wave height comparisons in figure 6 show good agreements between data and model results and also show the smoother wave height distributions than that in the monochromatic wave case.

For the most obliquely incident wave cases, fairly good agreements are also obtained from the model/data comparisons. Both measurement and numerical

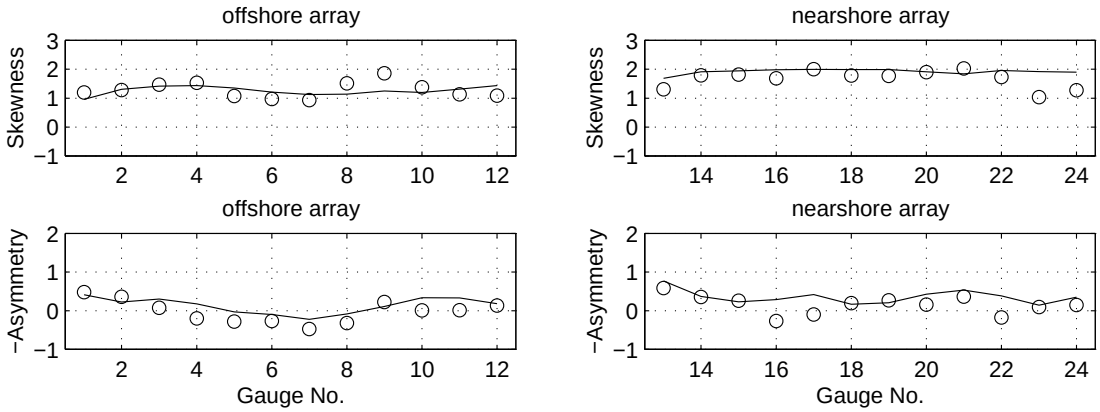


**Fig. 7. Comparisons of skewness and asymmetry (Case 14).**

results show that the locations of maximum wave heights caused by wave focusing shift to the right or left hand side in both offshore array and nearshore array in the cases of the obliquely incident waves.

Kirby and Dalrymple (1994) state that the models based on Stokes theory becomes invalid when the Ursell number exceeds 40. For the cases with a long period and a large wave height, $T = 15s, H = 0.98m$, for example, the Ursell number is nearly 40 at offshore array and about 200 at the nearshore array. The Stockes wave models are invalid for this case. To present the capability of the present model to calculate nonlinear waves, the data/model comparisons of skewness and asymmetry of waves are made for strong nonlinear wave cases. Figure 7 shows the good agreements in the comparisons of skewness and asymmetry between the numerical results and the measurements in Case 14.

## CONCLUSION

The curvilinear Boussinesq model based on the fully nonlinear equations is further improved by adding the wave breaking term, Smagorinsky subgrid mixing term and parameters used for the slot technique into the model. A TMA spectral wave maker is implemented for simulations of irregular waves. The improvements make the curvilinear model applicable to more practical computations in irregular shaped domains. As a practical application, wave simulations in Ponce de Leon Inlet are conducted in the paper. Model/Data comparisons are made and fairly good agreements are obtained.

## ACKNOWLEDGMENTS

This work was sponsored by National Oceanographic Partnership Program (NOPP). The authors would like to express their appreciation to Zeki Demirbilek and Jarrell Smith, U.S. Army Corps of Engineering, who supplied the data of Ponce de Leon Inlet.

## REFERENCES


Brackbill, J. U. and Saltzman, J. S., 1982, Adaptive zoning for singular problems in two dimensions, *J. Comput. Phys.*, 46, 342-368.

Chen, Q., Dalrymple, R.A., Kirby, J. T., Kennedy, A. and Haller M. C., 1999, Boussinesq modeling of a rip current system, *Journal of Geophysical Research*, 104, C9, 20617-20637.

Karambas, T. V. and Koutitas, C. A., 1992, A breaking wave propagation model based on the Boussinesq equations, *Coastal Eng.*, 18 1-19.

Kennedy, A. B., Chen, Q., Kirby, J. T., and Dalrymple, R. A., 2000, Boussinesq modeling of wave transformation, breaking, and runup, I, 1D, *J. Waterw. Port Coastal Ocean Eng.*, 126, 39-47.

Kirby, J. T. and Dalrymple, R. A., 1994, Combined Refraction/Diffraction Model REF/DIF 1, Version 2.5. Documentation and User's Manual, Research Report No.CACR-94-22, Center for Applied Coastal Research, Department of Civil Engineering, University of Delaware, Newark.

Li, Y. S., Liu, S. X., Yu, Y. X. and Lai, G. Z., 1999, Numerical modeling of Boussinesq equations by finite element method, *Coastal Eng.*, 37, 97-122.

Li, Y. S. and Zhan, J. M., 2001, Boussinesq-type model with boundary-fitted coordinate system, *J. Waterw. Port Coastal Ocean Eng.*, 127, 152-160.

Madsen, P. A., and Sørensen, O. R., 1992, A new form of the Boussinesq equations with improved linear dispersion characteristics, 2, A slowly varying bathymetry, *Coastal Eng.*, 18, 183-204.

Madsen, P. A., Sørensen, and Schäffer, 1997, Surf zone dynamics simulated by a Boussinesq model, I, Model description and cross-shore motion of regular waves, *Coastal Eng.*, 32, 255-287.

Nwogu, O., 1993, Alternative form of Boussinesq equations for nearshore wave propagation, *J. Waterw. Port Coastal Ocean Eng.*, 119, 618-638.

Schäffer, H. A., Madsen, P. A., and Deigaard, R. A., 1993, A Boussinesq model for waves breaking in shallow water, *Coastal Eng.*, 20, 185-202.

Shi, F., Dalrymple, R. A., Kirby, J. T., Chen, Q. and Kennedy, A., 2001, A fully nonlinear Boussinesq model in generalized curvilinear coordinates, *Coastal Eng.*, 42, 337-358.

Sørensen O. R. and Sørensen L. S., 2000, Boussinesq type modelling using unstructured finite element technique, *Proc. 27 Int. Conf. Coastal Eng.*, Vol 1, 190-202.

Smith, S. J. and Harkins, G. S., 1997, Numerical wave model evaluations using laboratory data, *Ocean wave measurement and analysis*, Vol 1, 271-285.

Wei, G. & Kirby, J. T., Grilli, S. T. and Subramanya, R., 1995, A fully nonlinear Boussinesq model for surface waves, Part 1, Highly nonlinear unsteady waves, *J. Fluid Mech.*, 294, 71-92.

Wei, G., Kirby, J. T. and Sinha, A., 1999,Generation of waves in Boussinesq models using a source function method, *Coastal Eng.*, 36, 271-299, 1999.